ELSEVIER

International Journal of Solids and Structures 41 (2004) 3243–3253

INTERNATIONAL JOURNAL OF SOLIDS and STRUCTURES

www.elsevier.com/locate/ijsolstr

Evaluation of interface strength of micro-dot on substrate by means of AFM

Hiroyuki Hirakata [a,*], Takayuki Kitamura [a], Yoshitake Yamamoto [b]

[a] *Department of Engineering Physics and Mechanics, Kyoto University, Yoshida-honmachi, Sakyo-ku, Kyoto 606-8501, Japan*
[b] *Graduate School of Engineering Physics and Mechanics, Kyoto University, Kyoto 606-8501, Japan*

Received 17 April 2003; received in revised form 12 December 2003

Available online 4 February 2004

Abstract

Using atomic force microscopy (AFM), we have developed an experimental method for evaluating interface strength of a small dot on a substrate. This technique is applied to tungsten (W) dots of micrometer size on a silicon (Si) substrate. The diamond tip is dragged horizontally along the Si surface and the load is applied to the side edge of the W dot at a constant displacement rate. Both the lateral and the vertical load and displacement are continuously monitored during the test. Results show that after the tip hits the W dot, the lateral load, F_l, increases almost in proportion to the lateral displacement, δ_l. The W dot is abruptly separated from the substrate along the interface, and the apparent fracture energy of the interface, E_d, is successfully evaluated.

Keywords: Delamination; Micro-dot; Atomic force microscopy; Interface strength; Micro-material; Micro-mechanics

1. Introduction

Because a micro-electronic device consists of various micro-components, there are many bi-material interfaces. Stress concentration at the interface due to the deformation mismatch sometimes causes delamination, which brings about fatal malfunction of the device. It is necessary, therefore, to evaluate the interface strength between the micro-component and the substrate.

Several techniques such as the scratch test (Baba et al., 1986; Lee et al., 1990; Venkataraman et al., 1996), the indentation test (Marshall and Evans, 1984; Rossington et al., 1984), the peeling test (Kim et al., 1978; Kinloch et al., 1994) and the topple test (Butler, 1970) are often used to evaluate the interface strength between a thin film and a substrate, since they are simple and easy to conduct. In recent years, more quantitative methods such as the blister test (Jensen, 1991; Jensen and Thouless, 1993), modified indentation tests (de Boer and Gerberich, 1996a,b; Vlassak et al., 1997; Kriese et al., 1999a,b; Begley et al., 2000),

* Corresponding author. Tel.: +81-75-753-5192; fax: +81-75-753-5256.
E-mail address: hirakata@kues.kyoto-u.ac.jp (H. Hirakata).

0020-7683/$ - see front matter © 2004 Elsevier Ltd. All rights reserved.
doi:10.1016/j.ijsolstr.2004.01.011

the modified scratch test (de Boer et al., 1997), tests using residual stress in the film itself or in an adjacent layer (Bagchi et al., 1994; Bagchi and Evans, 1996; Zhuk et al., 1998; Hay et al., 2001; Buchwalter, 2001; Kinbara et al., 1998), a test using electro-static force (Yang et al., 1997), the four-point flexure test (Dauskardt et al., 1998; Lane et al., 2000) and others (Kamiya et al., 2002; Xie and Sitaraman, 2003; Volinsky et al., 2003) have been proposed. We proposed an evaluation method for initiation criterion of an interface crack due to the free-edge effect on the basis of fracture mechanics, and its validity was examined experimentally (Kitamura et al., 2002, 2003). On the other hand, the stress-concentrated region on an interface, which dominates interface delamination, is affected by the length scale (Becker et al., 1997; Kitamura et al., 2003). The delamination behavior might be influenced by not only the thickness but also the size of film. Hence, it is important to elucidate the effect of length scale on the delamination. However, the most of the above methods can be applied only to layered materials that extend two-dimensionally; few techniques (de Boer et al., 1997; Kamiya et al., 1998) have been developed to evaluate the interface strength of a micro-component, of which the three-dimensional scale is small, on a substrate. This is due to the difficulty in applying effective load on the micro-component and in accurately measuring the displacement during the interface fracture.

In this study, an experimental method for evaluating the interface strength between a micro-component and a substrate is developed using a modified atomic force microscopy (AFM), which can control and measure precisely the load and the tip displacement. This technique is applied to tungsten (W) dots of several micrometers across on a silicon (Si) substrate.

2. Experimental procedure

2.1. Specimen preparation

Fig. 1 shows the schematic illustration of the specimens tested. A square W dot of 5 μm × 5 μm and a circular W dot of ∅2.5 μm are deposited on a Si substrate, and these are denoted as specimens A and B, respectively. The effect of adhesion area on the delamination behavior is examined by the specimens so that the adhesion area of the former is about four times that of the latter. The height of each dot is 0.1 μm. The reasons why the W/Si system has been selected in this study are:

(1) W and Si have high yield stress.
(2) The W/Si interface is expected to show brittle delamination behavior due to the high stiffness of both W and Si.
(3) W is an important material in micro-electronic devices.

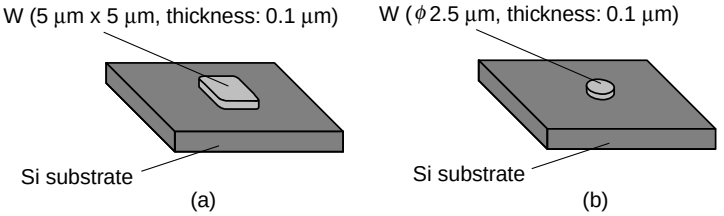

Fig. 1. Specimens of W dot on Si substrate: (a) specimen A and (b) specimen B.

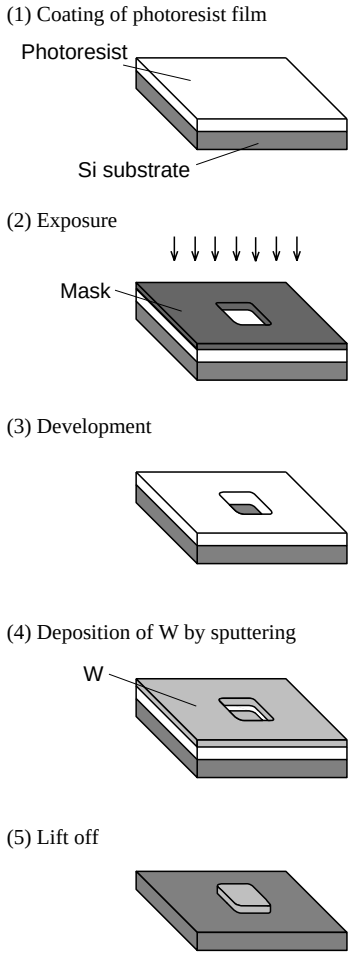

Fig. 2. Fabrication procedure of specimen.

The fabrication procedure of the specimens, which is schematically illustrated in Fig. 2, is explained below.

(1) A Si wafer (thickness: 550 μm, surface: (1 0 0) plane) is cleaned by ultrasonic vibration with organic solvents (acetone and isopropyl alcohol). Then, a photoresist film with the thickness of about 1 μm is deposited by spin-coating.
(2) The plate surface (except the part where the W dot will be deposited) is covered with a patterned mask. The specimen is then exposed to ultraviolet radiation.
(3) The exposed part of the photoresist film is removed with developer.
(4) After reducing the pressure to 2.3×10^{-4} Pa at room temperature, the 0.1-μm thick W film is sputtered onto the specimen in 0.8-Pa argon (Ar).
(5) The photoresist film with the W film is removed with pyrrolidone (lifted off).

The AFM images of specimen A are shown in Fig. 3. The corners of the square dot are round as shown in Fig. 3(a). A magnified view of the edge (Fig. 3(b)) reveals that the roughness of the W dot edge is less than

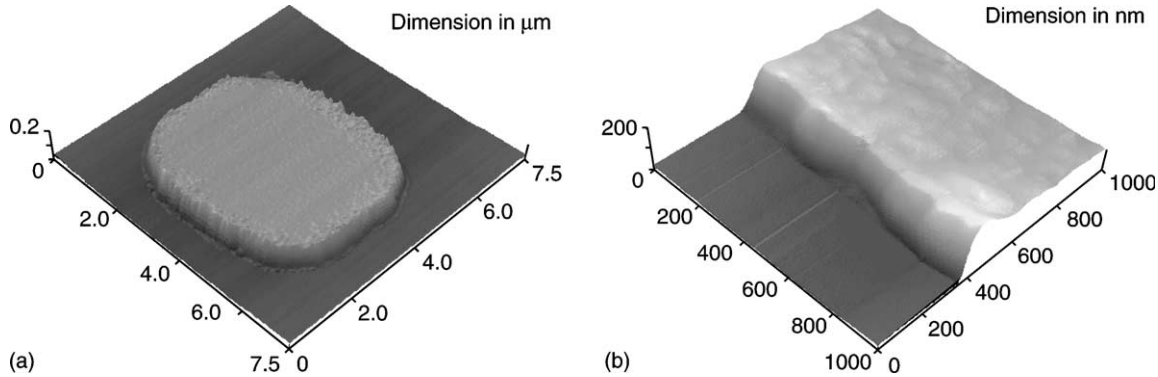

Fig. 3. AFM images of specimen A: (a) entire view and (b) magnified view of specimen edge.

0.1 μm, and there is slight unevenness on the dot surface near the edge that was introduced during the lift-off process.

2.2. Testing apparatus and loading system

Fig. 4 shows the testing apparatus and the loading system. A special loading apparatus, which can control precisely the lateral displacement of the tip at a resolution of 4 nm, is attached to the AFM. The apparatus consists of three force/displacement transducers, each of which has two fixed outer plates and a spring-suspended center plate. The loading tip is attached to the center plate of the middle transducer. The normal force, F_n, of the tip is electrostatically generated by applying a voltage between the center and the lower plates in the middle transducer, and the resulting normal displacement, δ_n, is detected by change in capacitance. The side transducers generate the lateral force, F_l, in the same manner, and control the lateral displacement, δ_l, using the capacitance signal.

The loading tip is positioned at the surface of the Si substrate near the W dot at first, and it is dragged horizontally along the Si surface at a constant rate of displacement, v, as shown in Fig. 5. F_n is kept constant during the test. Then, the load is directly applied to the side edge of the dot. The angle of the tip, which is tetrahedral in shape, is adjusted so that one of the side surfaces is parallel to the W dot edge (Fig. 5).

The tests are conducted with several combinations of F_n (1500–2200 μN) and v (20, 100 nm/s) at room temperature in an air environment. The test conditions and the adhesion area, A_d, are summarized in Tables 1 and 2, respectively. The fracture surface of each specimen is observed by AFM after the test.

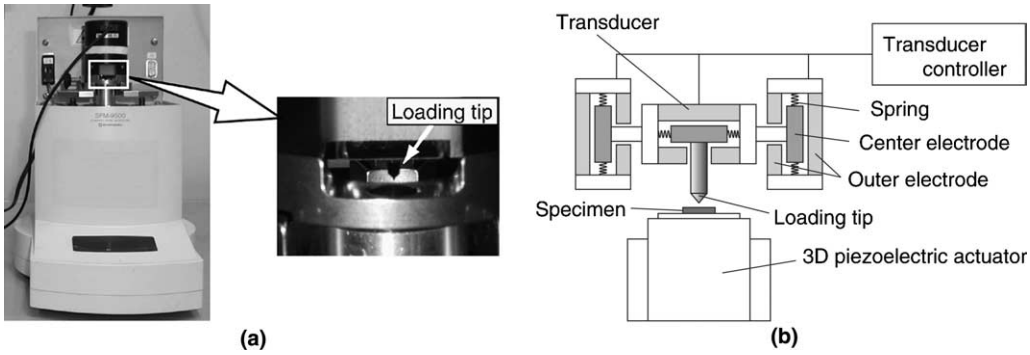

Fig. 4. Testing system: (a) photograph of testing apparatus and (b) schematic illustration of testing system.

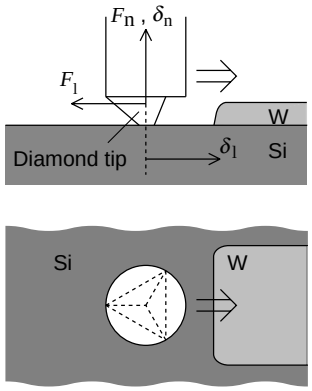

Fig. 5. Schematic illustration explaining the loading in the tests.

Table 1
Test condition

	Specimen type	Normal force F_n, μN	Lateral displacement rate v, nm/s
A-1	A	1700	100
A-2	A	1700	100
A-3	A	1700	100
A-4	A	1700	20
A-5	A	2200	100
A-6	A	2200	100
B-1	B	1500	100
B-2	B	1500	100
B-3	B	1500	100
B-4	B	1500	100
B-5	B	1500	100
B-6	B	1500	100
B-7	B	1500	20
B-8	B	1500	20
B-9	B	1500	20
B-10	B	1500	20
B-11	B	2000	20

3. Results

Fig. 6 shows the AFM image of the fracture surface of specimen A tested under $F_n = 1700$ μN and $v = 100$ nm/s. The region indicated by the dashed line designates the place where the W dot was located. The fracture clearly takes place along the interface between the W dot and the Si substrate. In the tests under conditions of $F_n < 1700$ μN, the tip ran onto the W dot and the interface fracture did not take place.

Figs. 7(a) and (b) show the relationships between the lateral force, F_l, and lateral displacement, δ_l, and the normal displacement, δ_n, and time, t. It is clear that F_l increases at an early stage and remains constant up to about $\delta_l = 3$ μm (“a” in the figure). After point “a,” F_l increases up to point “b,” then shows sharp drop. Based on the F_l–δ_l relation, the process is divided into the following four regions.

Region I: Region where F_l is constant (before point “a”).

Region II: Region where F_l increases (from point “a” to point “b”).

Table 2
Adhesion area (A_d)

	Specimen type	Adhesion area A_d, μm^2
A-1	A	23.0
A-2	A	22.1
A-3	A	21.0
A-4	A	21.7
A-5	A	25.8
A-6	A	24.6
B-1	B	5.92
B-2	B	8.32
B-3	B	6.39
B-4	B	6.46
B-5	B	6.41
B-6	B	6.11
B-7	B	5.83
B-8	B	5.84
B-9	B	5.69
B-10	B	7.22
B-11	B	8.78

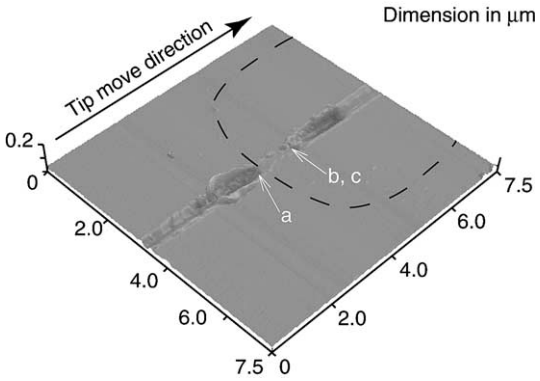

Fig. 6. AFM image of fracture surface of specimen A ($F_n = 1700$ μN and $v = 100$ nm/s).

Region III: Region where F_l decreases rapidly (from point "b" to point "c").

Region IV: Region where F_l comes back to the level in Region I (after point "c").

The locations at points "a," "b" and "c" on the fracture surface are marked by the arrows in Fig. 6. A ditch is observed on the Si surface in Region I. Referring to the decrease in δ_n at the beginning shown in Fig. 7(b), it is obvious that the tip scratches the Si substrate in this region. Since F_l begins to increase at point "a," the tip hits the edge of the W dot at point "a" as schematically illustrated in Fig. 8. In other words, the load is applied to the dot in Region II. Attention must be paid to the fact that δ_n also increases in Region II and that the ditch on the fracture surface disappeared after point "a." The tip contacts only the W dot in almost all of Region II. The abrupt decrease of F_l and δ_n in Region III indicates the separation of the W dot from the Si substrate. In Region IV, the tip scratched the Si substrate again.

Fig. 9 shows the relationship between F_l and δ_l in specimen B tested under $F_n = 1500$ μN and $v = 100$ nm/s. The delamination behavior is similar to that in specimen A. The separated W dot was found after the

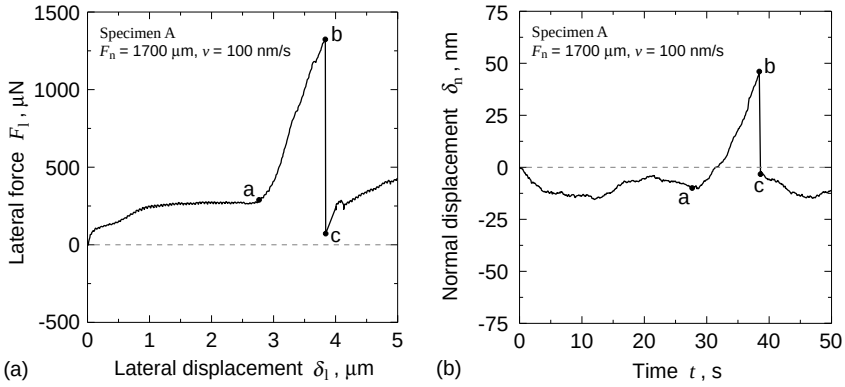

Fig. 7. Relationships between lateral force and lateral displacement, and normal displacement and time in specimen A ($F_n = 1700$ μN and $v = 100$ nm/s). (a) F_l–δ_l curve (b) δ_n–t curve.

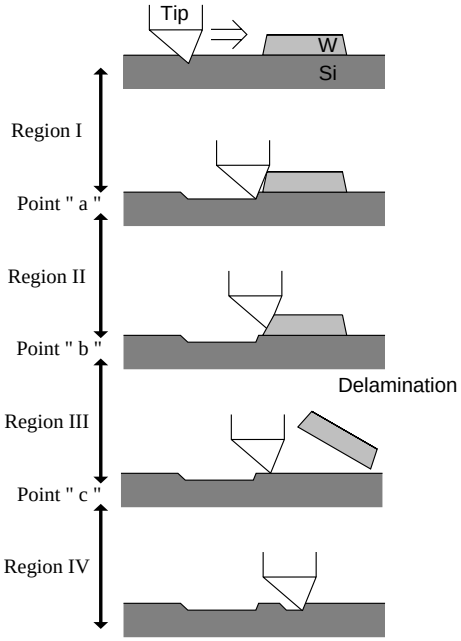

Fig. 8. Schematic illustration of delamination process.

delamination test of specimen B, and it was carefully examined by means of AFM. Fig. 10 shows the part where the tip pushed the W dot. As seen in the figure, there is very little plastic deformation.

4. Discussion

The peak load, F_{lC} (the lateral force at point "b"), and the apparent delamination stress, τ_C, which is defined as F_{lC}/A_d, is shown in Table 3. The F_{lC} of specimen A is much higher than that of specimen B, while

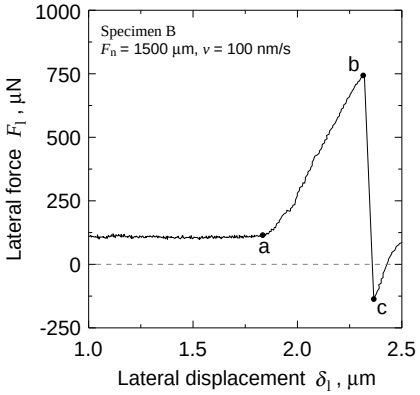

Fig. 9. Relationship between lateral force and lateral displacement in specimen B ($F_n = 1500$ μN and $v = 100$ nm/s).

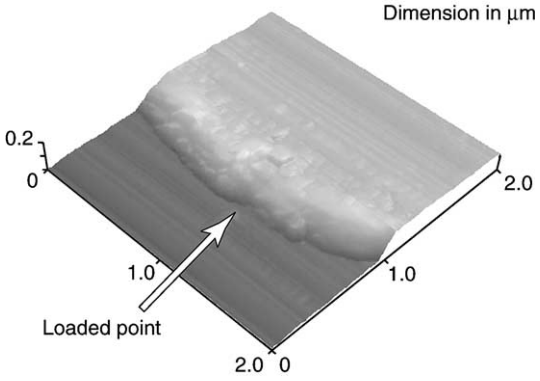

Fig. 10. AFM image of delaminated W dot from specimen B ($F_n = 1500$ μN and $v = 100$ nm/s).

the τ_C of specimen A is much lower than that of specimen B. Therefore, F_{lC} and τ_C are not good criteria for evaluating the interface toughness.

The apparent delamination energy is evaluated assuming that all the elastic strain energy stored is consumed during the delamination of the W dot from the Si substrate. In some tests, the specimen is unloaded just before the delamination. In the case of specimen A, F_l decreases at the slope of about 2100 N/m during the unloading, as shown in Fig. 11. Thus, the stored elastic energy at the delamination, E_e can be estimated as the area of the triangle αbβ (the gray region) in the schematic F_l–δ_l diagram, Fig. 12. In this study, the apparent delamination energy, E_d, is defined as E_e/A_d. This is "apparent" because the energy is consumed for the plastic deformation of the W dot. Although it must be estimated by deformation analysis to make a precise evaluation, it is out of scope of this paper. The stress concentration near the interface edge may dominate the delamination; however, it is too complex to analyze precisely in this case. As a result, we use E_d as a first step in the evaluation.

The values of E_d in specimens A and B are shown in Table 3; E_d is 16–21 J/m^2 in specimen A and 15–29 J/m^2 in specimen B. Although there is still uncertain scatter in the E_d values, especially in specimen B, the dependence of E_d on A_d and on the test condition is relatively small. This signifies that E_d is a good candidate for the criterion to evaluate the interface strength between the W dot and the Si substrate.

Table 3
Delamination load (F_{lC}), delamination stress (τ_C) and delamination energy (E_d)

	Specimen type	Delamination load F_{lC}, μN	Delamination stress τ_C, MPa	Delamination energy E_d, J/m^2
A-1	A	1252	54.4	16.0
A-2	A	1240	56.2	16.3
A-3	A	1286	61.3	18.5
A-4	A	1293	59.6	18.1
A-5	A	1512	58.6	20.8
A-6	A	1469	59.6	20.5
B-1	B	818	138.2	26.9
B-2	B	739	88.9	15.6
B-3	B	852	133.4	27.0
B-4	B	736	113.9	20.0
B-5	B	805	125.6	24.0
B-6	B	762	124.7	22.6
B-7	B	668	114.7	18.2
B-8	B	741	126.8	22.3
B-9	B	830	145.9	28.8
B-10	B	677	93.7	15.1
B-11	B	874	99.5	20.7

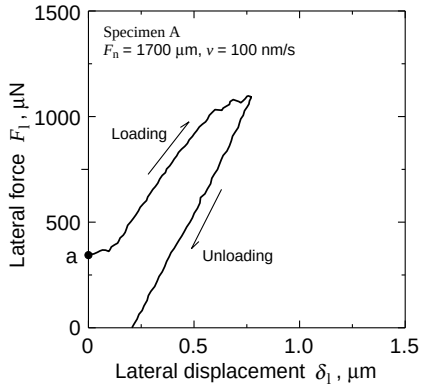

Fig. 11. Relationship between lateral force and lateral displacement in specimen A during unloading ($F_n = 1700$ μN and $v = 100$ nm/s).

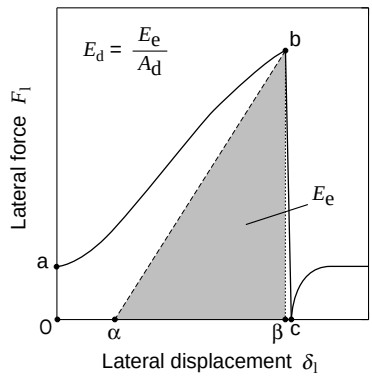

Fig. 12. Schematic illustration of delamination energy.

5. Conclusions

The results obtained are summarized as follows:

(1) An experimental method for evaluating the interface strength of a micro-dot on a substrate was developed using a modified AFM, which can control and measure precisely the load and the tip displacement. This technique was applied to W dots of several micrometers across on a Si substrate.
(2) A square W dot of 5 μm × 5 μm (specimen A) and a circular W dot of ∅2.5 μm (specimen B) on the Si substrate were prepared. The diamond tip was dragged horizontally along the Si surface and a load was applied to the side edge of the W dot at a constant displacement rate.
(3) After the tip hit the W dot, the lateral force, F_l, increased almost in proportion to the lateral displacement, δ_l. Then, the W dot was abruptly separated from the substrate along the interface.
(4) The peak load, F_{lC}, and the apparent delamination stress, τ_C, strongly depended on the adhesion area of the specimen.
(5) The apparent delamination energy, E_d, was successfully evaluated as 16–21 J/m^2 in specimen A and 15–29 J/m^2 in specimen B, and is a good candidate for the criterion to evaluate the interface strength between the W dot and the Si substrate.

Acknowledgement

This research is partly supported by grant-in-aid for Scientific Research of (B) (no.14350055) of Japan Society of the Promotion of Science.

References

Baba, S., Kikuchi, A., Kinbara, A., 1986. A microtribometer for measurement of friction and adhesion of coatings. Journal of Vacuum Science and Technology A 4, 3015–3017.

Bagchi, A., Evans, A.G., 1996. Measurements of the debond energy for thin metallization lines on dielectrics. Thin Solid Films 286, 203–212.

Bagchi, A., Lucas, G.E., Suo, Z., Evans, A.G., 1994. A new procedure for measuring the decohesion energy for thin ductile film on substrates. Journal of Materials Research 9, 1734–1741.

Becker Jr., T.L., McNancy, J.M., Cannon, R.M., Ritchie, R.O., 1997. Limitations on the use of the mixed-mode delaminating beam test specimen: effect of the size of the region of K-dominance. Mechanics of Materials 25, 291–308.

Begley, M.R., Mumm, D.R., Evans, A.G., Hutchinson, J.W., 2000. Analysis of a wedge impression test for measuring the interface toughness between films/coatings and ductile substrates. Acta Materialia 48, 3211–3220.

Buchwalter, L.P., 2001. Relative adhesion measurement for thin film microelectronic structures. Part II. In: Adhesion Measurement of Films and Coatings, vol. 2. VSP, Netherlands, pp. 19–47.

Butler, D.W., 1970. A simple film adhesion comparater. Journal of Physics E: Scientific Instruments 3, 979–980.

Dauskardt, R.H., Lane, M., Ma, Q., Krishna, N., 1998. Adhesion and debonding of multi-layer thin film structures. Engineering Fracture Mechanics 61, 141–162.

de Boer, M.P., Gerberich, W.W., 1996a. Microwedge indentation of the thin film fine line—I. Mechanics. Acta Materialia 44, 3175–3196.

de Boer, M.P., Gerberich, W.W., 1996b. Microwedge indentation of the thin film fine line—II. Experiment. Acta Materialia 44, 3177–3187.

de Boer, M.P., Kriese, M.D., Gerberich, W.W., 1997. Investigation of a new fracture mechanics specimen for thin film adhesion measurement. Journal of Materials Research 12, 2673–2685.

Hay, J.C., Liniger, E.G., Liu, X.H., 2001. Measurements of interfacial fracture energy in microelectronic multifilm applications. In: Adhesion Measurement of Films and Coatings, vol. 2. VSP, Netherlands, pp. 205–217.

Jensen, H.M., 1991. The blister test for interface toughness measurement. Engineering Fracture Mechanics 40, 475–486.

Jensen, H.M., Thouless, M.D., 1993. Effect of residual stresses in the blister test. International Journal of Solids and Structures 30, 779–795.

Kamiya, S., Takahashi, H., Saka, M., Abe, H., 1998. Direct measurement of the adhesive fracture resistance of CVD diamond particles. Journal of Electronic Packaging 120, 367–371.

Kamiya, S., Kimura, H., Yamanobe, K., Saka, M., Abe, H., 2002. A new systematic method of characterization for the strength of thin films on substrates-evaluation of mechanical properties by means of 'film projection'. Thin Solid Films 414, 91–98.

Kim, Y.H., Chaug, N.J., Chou, N.J., Kim, J., 1978. Adhesion of titanium thin film to oxide substrates. Journal of Vacuum Science and Technology A 5, 2890–2893.

Kinbara, A., Kusano, E., Kamiya, T., Kondo, I., Takenaka, O., 1998. Evaluation of adhesion strength of Ti films on Si(1 0 0) by the internal stress method. Thin Solid Films 317, 165–168.

Kinloch, A.J., Lau, C.C., Williams, J.G., 1994. The peeling of flexible laminated. International Journal of Fracture 66, 45–70.

Kitamura, T., Shibutani, T., Ueno, T., 2002. Crack initiation at free edge of interface between thin films in advanced LSI. Engineering Fracture Mechanics 69, 1289–1299.

Kitamura, T., Hirakata, H., Itsuji, T., 2003. Effect of residual stress on delamination from interface edge between nano-films. Engineering Fracture Mechanics 70, 2089–2101.

Kriese, M.D., Gerberich, W.W., Moody, N.R., 1999a. Quantitative adhesion measures of multilayer films. Part I: Indentation mechanics. Journal of Materials Research 14, 3007–3018.

Kriese, M.D., Gerberich, W.W., Moody, N.R., 1999b. Quantitative adhesion measures of multilayer films. Part II: Indentation of W/Cu, W/W, Cr/W. Journal of Materials Research 14, 3019–3026.

Lane, M., Dauskardt, R.H., Krishna, N., Hashim, I., 2000. Adhesion and reliability of copper interconnects with Ta and TaN barrier layers. Journal of Materials Research 15, 203–211.

Lee, G.H., Cailler, M., Kwon, S.C., 1990. Adhesion studies of magnetron-sputtered copper films on nickel substrates: effects of substrate surface pretreatments. Thin Solid Films 185, 21–33.

Marshall, D.B., Evans, A.G., 1984. Measurement of adherence of residually stressed thin films by indentation. I. Mechanics of interface delamination. Journal of Applied Physics 56, 2632–2638.

Rossington, C., Evans, A.G., Marshall, D.B., Khuri-Yakub, B.T., 1984. Measurement of adherence of residually stressed thin films by indentation. II. Experiments with ZnO/Si. Journal of Applied Physics 56, 2639–2644.

Venkataraman, S., Kohlstedt, D.L., Gerberich, W.W., 1996. Continuous microscratch measurements of the practical and true works of adhesion for metal/ceramic systems. Journal of Materials Research 11–12, 3133–3145.

Vlassak, J.J., Drory, M.D., Nix, W.D., 1997. A simple technique for measuring the adhesion of brittle films to ductile substrates with application to diamond-coated titanium. Journal of Materials Research 12, 1900–1910.

Volinsky, A.A., Moody, N.R., Gerberich, W.W., 2003. Fiducial mark and CTOA estimates of thin films adhesion. International Journal of Fracture 119/120, 431–439.

Xie, W., Sitaraman, S.K., 2003. An experimental technique to determine critical stress intensity factor for delamination initiation. Engineering Fracture Mechanics 70, 1193–1201.

Yang, H.S., Brotzen, F.R., Callahan, D.L., 1997. Electrostatic adhesion testing of electronic metallizations. Review of Scientific Instruments 68, 2542–2545.

Zhuk, A.V., Evans, A.G., Hutchinson, J.W., Whitesides, G.M., 1998. The adhesion energy between polymer thin films and self-assembled monolayers. Journal of Materials Research 13, 3555–3564.